Quaternary Science Reviews 134 (2016) 92–99

Contents lists available at ScienceDirect

Quaternary Science Reviews

journal homepage: www.elsevier.com/locate/quascirev

Rapid human-induced landscape transformation in Madagascar at the end of the first millennium of the Common Era

Stephen J. Burns [a, *], Laurie R. Godfrey [b], Peterson Faina [c], David McGee [d], Ben Hardt [d], Lovasoa Ranivoharimanana [c], Jeannot Randrianasy [c]

[a] Department of Geosciences, 611 North Pleasant Street, University of Massachusetts, Amherst, MA 01003, USA
[b] Department of Anthropology, 240 Hicks Way, University of Massachusetts, Amherst, MA 01003, USA
[c] Département de Paléontologie et d'Anthropologie Biologique, Faculté des Sciences, B.P 906 – 101 Antananarivo, Madagascar
[d] Department of Earth, Atmospheric and Planetary Sciences, Massachusetts Institute of Technology, 77 Massachusetts Avenue, Cambridge, MA 02139, USA

ARTICLE INFO

Article history:
Received 23 October 2015
Received in revised form
8 January 2016
Accepted 12 January 2016
Available online xxx

Keywords:
Paleoecology
Paleoclimatology
Stable isotopes
Speleothems
Madagascar

ABSTRACT

The environmental impact of the early human inhabitants of Madagascar remains heavily debated. We present results from a study using two stalagmites collected from Anjohibe Cave in northwestern Madagascar to investigate the paleoecology and paleoclimate of northwestern Madagascar over the past 1800 years. Carbon stable isotopic data indicate a rapid, complete transformation from a flora dominated by C_3 plants to a C_4 grassland system. This transformation is well replicated in both stalagmites, occurred at 890 CE and was completed within one century. We infer that the change was the result of a dramatic increase in the use of fire to promote the growth of grass for cattle fodder. Further, stalagmite oxygen isotope ratios show no significant variation across the carbon isotope excursion, demonstrating that the landscape transformation was not related to changes in precipitation. Our study illustrates the profound impact early inhabitants had on the environment, and implies that forest loss was one trigger of megafaunal extinction.

1. Introduction

Considerable controversy remains over the timing, causes and magnitude of forest and woodland loss in Madagascar (McConnell and Kull, 2014). For much of the past century the prevailing view was that prior to human arrival forest and woodland covered 90% of the island (Humbert, 1927), and that the loss of Madagascar's forests was due to human activity (Perrier de la Bâthie, 1921). Recent studies, however, suggest that Madagascar's grasslands are a natural part of the island's ecosystem (Burney, 1987; Quéméré et al., 2012) and may even date to the late Miocene (Bond et al., 2008). Indeed, some authors question the entire narrative of extensive alteration of the landscape by early human activity (Klein, 2002; Kull, 2000). Whether forest loss was the result of early human activity (Gade, 1996), was post-Colonial (Jarosz, 1993) or was, in fact, not significant (Klein, 2002) also has important implications for the causes of the decline and ultimate disappearance of Madagascar's endemic megafauna, which mainly occurred prior to European contact (Burney et al., 2004; Crowley, 2010). Answering these questions is difficult because there are few high-resolution, well-dated studies of Madagascar's paleoclimate and paleoecology.

Speleothems, calcium carbonate cave deposits, offer an opportunity to investigate both ecosystem and climate change in the same archive via stable carbon and oxygen isotope ratios, respectively. Carbon isotope ratios are sensitive to the ratio of surface flora that utilize the C_3 (woody taxa) versus C_4 (grasses) photosynthetic pathways. In the tropics, the oxygen isotope ratio of precipitation is, empirically and mechanistically, strongly correlated with the amount of precipitation, a signal that is captured in the oxygen isotope ratios of speleothem calcite. Speleothems also offer unusually robust chronological control through disequilibrium U-series dating techniques. To investigate the recent environmental and climate history of Madagascar, we collected two actively growing stalagmites, M14-AB2 and M14-AB3, from Anjohibe Cave (15.54°S, 46.89°E, 131 masl) in northwestern Madagascar in 2014.

2. Setting

Ajohibe Cave is part of a karst system formed within the Eocene

* Corresponding author.
E-mail address: sburns@geo.umass.edu (S.J. Burns).

http://dx.doi.org/10.1016/j.quascirev.2016.01.007
0277-3791/

limestone plateau (Besairie and Collignon, 1972) of northwestern Madagascar (Fig. 1). Anjohibe ('big cave' in Malagasy) consists of 5.3 km of cave passages with over two dozen openings (Burney et al., 1997). Samples AB2 and AB3 (Fig. 2) were taken ~1 km from the main entrance to the cave and approximately 400 m distant from one another (for a map of the cave see Burney et al., 1997). The samples were collected in October, at the end of the dry season, and there were very few active drips within the cave. Neither sample was beneath an active drip at the time of collection. Both samples appeared to be still actively or very recently growing, however, based on the clean, white calcite deposits on the top of the stalagmites.

The landscape overlying the cave is presently palm savannah (Fig. 1) with small patches of mesic forest in wetter areas (Burney et al., 1997). Rainfall in the region is highly seasonal. At the nearest weather station, Mahajanga, which is ~70 km from the cave, over 80% of the mean annual rainfall (1496 mm) occurs in the four month period from December through April. Mean monthly temperature varies 3.2 °C throughout the year, with an annual mean of 27.2 °C (data from http://www.ncdc.noaa.gov/data-access).

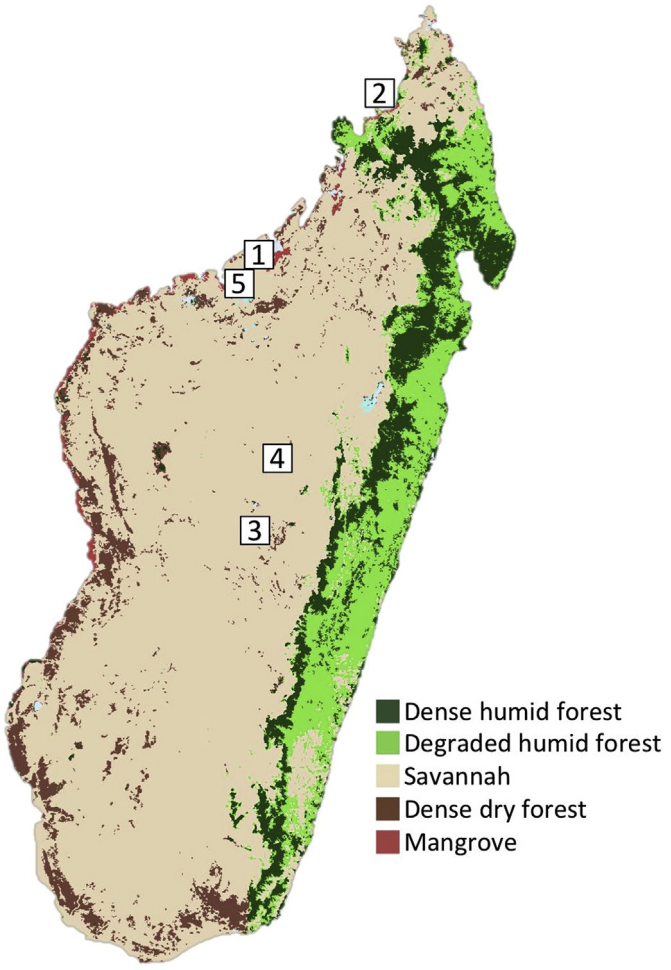

Fig. 1. Madagascar ecosystems and site location. This map shows the present distribution of major ecosystems in Madagascar (Mayaux et al., 2000) and the locations of the study area and lake study sites mentioned in the text: 1. Anjohibe Cave, 2. Lake Amparihibe (Burney et al., 2004), 3. Lake Tritrivakely (Gasse and Van Campo, 1998), 4. Lake Kavitaha (Burney, 1987) and 5. Lake Mitsinjo (Matsumoto and Burney, 1994).

Fig. 2. Sample photographs. Photograph with scale of cut and polished slabs of samples AB2 and AB3 showing internal layering.

3. Methods

The two speleothems were halved along the growth axis and subsampled along growth layers for radiometric dating using uranium-thorium (U–Th) techniques by multi-collector, inductively coupled plasma mass spectroscopy (MC-ICP-MS) (Cheng et al., 2013). Carbon and oxygen stable isotope ratios were measured on 266 samples from AB2 and 173 samples from AB3. Temporal resolution of the stable isotope time series is less than 10 years for all of M14-AB2 and M14-AB3. Age models (Fig. 3) were constructed using 8 age determinations from AB2 and 10 from AB3 (Table 1) and assuming an age for the top of each stalagmite of 2014 CE.

3.1. O and C stable isotope analyses

The stable oxygen and carbon isotope ratio measurements were

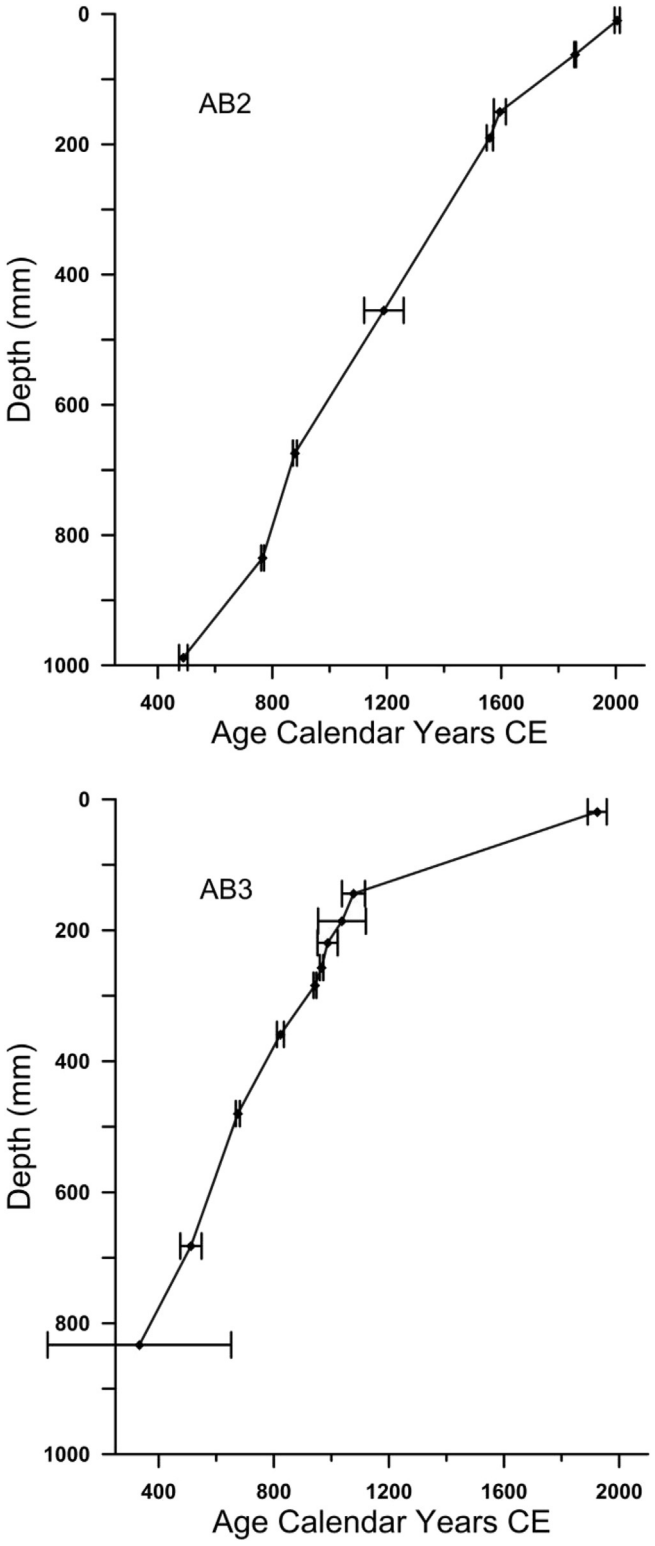

Fig. 3. Age-depth data. These plots show the U/Th age determinations with 2σ errors versus depth for each sample.

performed at the University of Massachusetts. Subsamples were microdrilled from a cut and polished slab every 0.5–01 mm along the central growth axis of the stalagmites. The sampling interval yields sub-decadal resolution throughout the record. The samples were analyzed in an on-line carbonate preparation system linked to a Finnigan Delta Plus XL ratio mass spectrometer. Results are reported as the per mil difference between sample and the Vienna Pee Dee Belemnite (VPDB) standard in delta notation where $\delta^{18}O = R_{sample}/R_{standard} - 1)^{*}1000$, and R is the ratio of the minor to the major isotope. Reproducibility of standard materials is 0.1‰ for $\delta^{18}O$ and 0.05‰ for $\delta^{13}C$.

3.2. U–Th dating

U–Th dating samples were prepared and analyzed at MIT. Samples weighing 25–210 mg were combined with a ^{229}Th–^{233}U–^{236}U tracer, digested, and purified via iron co-precipitation and ion exchange chromatography. Separate U and Th aliquots were analyzed using a Nu Plasma II-ES multi-collector ICP-MS equipped with a CETAC Aridus II desolvating nebulizer. Analyses were performed in static mode with ^{234}U and ^{230}Th measured on an ion counter and all other masses measured on Faraday cups. U and Th standard solutions bracketed each analysis to monitor mass bias and ion counter yield. CRM-112a was used to bracket U analyses, and an internally calibrated ^{229}Th–^{230}Th–^{232}Th standard (MITh-1) was used for Th. Tailing was assessed for each U standard and sample by measurement of half-masses (233.5, 234.5, 236.5) and mass 237, and tails were fit to a power law. Th tailing was measured once per day by measuring masses 229.5 and 230.5 in the MITh-1 standard. Tailing was consistently 1–2 ppm at 1 amu. Uranium hydride counts were also measured each day and were consistently 2–2.5 ppm. Ionization, transmission and detection efficiency was approximately 1% for both U and Th. MIT's isotope tracer is calibrated against the University of Minnesota's isotope tracer (Cheng et al., 2013) and standard HU-1. The laboratory's age determinations produce good agreement with ages from the Berkeley Geochronology Center in an intercomparison of young (<500 y) powder splits (McGee, unpublished data).

Reported isotope ratios uncertainties reflect propagated uncertainties from isotope ratio measurements, spike calibration and isotopic composition, instrument background, procedural blanks (assigned a 50% 2σ uncertainty), SEM yield drift, tailing and ^{233}UH counts on ^{234}U. Uncertainties on U and Th half-lives are not included, but would be insignificant relative to other uncertainties. Total procedural blanks ranged from 0.02 to 0.2 fg ^{230}Th in three of the four sample sets, with an anomalously high blank of 1.7 fg ^{230}Th in sample set 150206, and 30–300 pg ^{238}U for all four sample sets. The only sample for which the total uncertainty is increased by more than a decade due to the procedural blank is sample AB3-682 (512 ± 37 CE) due to the unusually high ^{230}Th blank in sample set 150206.

Ages were calculated using the ^{230}Th and ^{234}U half-lives of Cheng et al. (2013) and the ^{238}U half-life from Jaffey et al. (1971). Corrections for initial ^{230}Th assume an initial $^{230}Th/^{232}Th$ ratio of $17 \pm 8.5 \times 10^{-6}$ (atomic ratio). The mean value was determined from the construction of Osmond Type II isochrons from three samples at 62 mm depth in stalagmite M14-AB2 using Isoplot 4.15 (Ludwig, 1993), which gave an initial $^{230}Th/^{232}Th$ ratio of $17 \pm 4 \times 10^{-6}$ (Fig. 4). We chose to assign a relative uncertainty of 50% (2σ) to allow for temporal variability in the initial ratio. Two pieces of evidence suggest that this mean value and uncertainty are appropriate. First, the $^{230}Th/^{232}Th$ ratio from our youngest sample (AB2-9.5) is $26.6 \pm 1.0 \times 10^{-6}$, suggesting that the initial $^{230}Th/^{232}Th$ should be lower than this value. Second, an initial $^{230}Th/^{232}Th$ ratio greater than 11×10^{-6} is required to maintain stratigraphic order for samples AB3-144 through AB3-257. Similar constraints from stratigraphic order have been used to estimate initial $^{230}Th/^{232}Th$ ratios in previous studies (Cheng et al., 2000; McGee et al., 2012). Four samples have unusually low U concentrations and produce ages that are anomalously old (AB3-68, AB3-

Table 1
U–Th dating results.

Sample ID	Sample set	Distance from top (mm)	^{238}U (ng/g)[a]	± (2σ)	^{232}Th (pg/g)[a]	± (2σ)	$\delta^{234}U$ (per mil)[b]	± (2σ)	($^{230}Th/^{238}U$) (activity)	± (2σ)	$^{230}Th/^{232}Th$ (atomic $\times 10^{-6}$)	± (2σ)	Age (yr) (uncorrected)[c]	± (2σ)	Age (yr) (corrected)[d]	± (2σ)	$\delta^{234}U$ initial (per mil)[e]	± (2σ)	Year C.E. (corrected)[d]	± (2σ)
AB3-19	150713	19	10970	220	6120	120	2.3	1.2	0.001436	0.000013	41	0.4	156.3	1.5	91	33	2.3	1.2	1924	33
AB3-68	150713	68	140	3	1446	29	−5.8	2.8	0.01544	0.00034	24	0.4	1707	38	490	610	−5.8	2.8	1525	610
AB3-87	150713	87	175	4	574	12	−3.4	2.3	0.01445	0.00028	70	1.2	1593	31	1210	190	−3.4	2.3	805	190
AB3-144	150713	144	2078	42	1422	29	−2.3	1.4	0.009272	0.000094	215	2.2	1018	10	938	40	−2.3	1.4	1077	40
AB3-186	150713	186	2680	54	3773	76	−3.3	1.6	0.010395	0.000042	117	0.4	1143	5	978	83	−3.3	1.6	1037	83
AB3-219	150713	219	4644	93	2787	56	−3.4	1.6	0.009989	0.000046	264	1.1	1098	5	1028	35	−3.4	1.6	987	35
AB3-257	150713	257	6450	130	423	9	−3.7	1.5	0.009610	0.000048	2328	24	1057	6	1049	6	−3.7	1.5	966	6
AB3-284	150713	284	8550	170	444	10	−2.5	1.6	0.009817	0.000041	3000	27	1078	5	1072	5	−2.5	1.6	943	5
AB3-359	150730	359	7220	140	1488	30	0.4	1.8	0.011097	0.000052	855	4	1216	6	1192	12	0.4	1.8	823	12
AB3-480R	150730	480	4831	97	532	11	−0.4	1.8	0.012327	0.000063	1778	12	1353	7	1340	7	−0.4	1.8	675	7
AB3-682	150206	682	8370	170	609	25	0.4	1.1	0.01377	0.00033	3001	130	1511	37	1503	37	0.4	1.1	512	37
AB3-833	150206	833	1882	38	10250	210	0.9	1.2	0.02106	0.00061	61	2	2319	68	1680	320	0.9	1.2	335	320
AB2-9.5	150616	9.5	7940	160	1204	25	−9.1	1.4	0.0002539	0.0000099	26.6	1.0	28	1	10	9	−9.1	1.4	2005	9
AB2-62	150616	62	9160	180	496	11	−10.0	0.6	0.001484	0.000020	435.7	7.4	164	2	157	3	−10.0	0.6	1858	3
AB2-114	150616	114	183	4	485	11	−10.0	2.1	0.01252	0.00070	75.2	4.3	1387	78	1080	160	−10.0	2.1	935	160
AB2-150	150713	150	7950	160	2867	57	−12.8	1.4	0.004181	0.000018	184.1	0.7	463	2	420	21	−12.8	1.4	1595	21
AB2-190	150616	190	5560	110	1067	22	−3.0	1.3	0.004359	0.000036	360.8	3.3	478	4	455	11	−3.0	1.3	1560	11
AB2-455	150616	455	3561	71	4157	83	−7.8	1.2	0.008719	0.000054	118.6	0.7	963	6	825	69	−7.8	1.2	1190	69
AB2-556	150730	556	1096	22	274	6	−7.1	2.7	0.01076	0.00012	683.3	9.9	1188	14	1159	15	−7.1	2.7	856	15
AB2-674	150616	674	10710	220	281	7	−6.6	3.0	0.010318	0.000053	6252	94	1139	7	1136	7	−6.7	3.0	879	7
AB2-835	150616	835	8770	180	331	7	−3.8	0.5	0.011386	0.000042	4789	47	1253	5	1249	5	−3.8	0.5	766	5
AB2-988	150616	988	8220	160	943	19	0.4	7.9	0.014025	0.000084	1943	13	1540	15	1526	15	0.4	7.9	489	15
Isochron analyses																				
AB2-62L	150730	62	8730	180	4321	87	−0.3	1.7	0.002019	0.000036	64.8	1.1								
AB2-62R	150730	62	7300	150	2099	42	−7.9	1.8	0.001677	0.000030	92.6	1.6								
AB3-284L	150730	284	8450	170	1299	26	−0.5	1.8	0.013876	0.000071	1432.4	9.1								
AB3-284R	150730	284	10880	220	1404	28	−0.2	1.9	0.007362	0.000042	906.2	5.1								
AB3-480	150206	480	4007	80	757	26	1.3	1.2	0.011802	0.000644	993	61								
AB3-480L	150730	480	5190	100	1788	36	−0.9	1.9	0.012274	0.000070	565.3	3.2								

Notes:
Decay constants for ^{230}Th and ^{234}U are from Cheng et al. (2013); decay constant for ^{238}U is from Jaffey et al. (1971).

[a] Reported errors for ^{238}U and ^{232}Th concentrations are estimated to be ±1% due to uncertainties in spike concentration; analytical uncertainties are smaller.

[b] $\delta^{234}U = ([^{234}U/^{238}U]_{activity} - 1) \times 1000$.

[c] $[^{230}Th/^{238}U]_{activity} = 1 - e^{-\lambda 230 T} + (\delta^{234}U_{measured}/1000)[\lambda_{230}/(\lambda_{230} - \lambda_{234})](1 - e^{-(\lambda 230 - \lambda 234) T})$, where T is the age. "Uncorrected" indicates that no correction has been made for initial ^{230}Th.

[d] Ages are corrected for detrital ^{230}Th assuming an initial $^{230}Th/^{232}Th$ of $(17 \pm 8.5) \times 10^{-6}$.

[e] $\delta^{234}U_{initial}$ corrected was calculated based on ^{230}Th age (T), i.e., $\delta^{234}U_{initial} = \delta^{234}U_{measured}\ X\ e^{\lambda 234 * T}$, and T is corrected age.

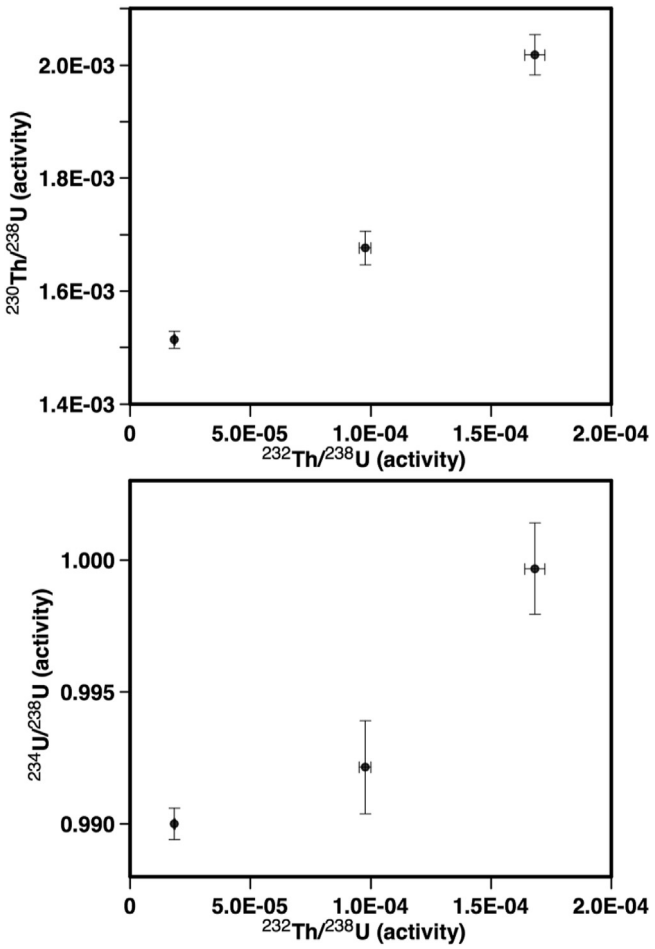

Fig. 4. Isochron data from sample AB2-62. The data indicate an initial $^{230}Th/^{232}Th$ atomic ratio of $17 \pm 4 \times 10^{-6}$. This value with an expanded uncertainty was used to calculate ages corrected for initial ^{230}Th for all samples.

87, AB2-114, AB2-556.) We interpret these horizons as having suffered diagenetic U loss and do not include them in the age models.

4. Results

Fig. 5 shows time series of oxygen and carbon isotope values in standard delta notation versus age for both stalagmites. The carbon isotope time series for our samples show relatively constant negative values from 500 CE to about 890 CE. For stalagmite AB2 the average $\delta^{13}C$ value over this time interval is −7.21‰, and for AB3 it is −8.77‰. The ~1.5‰ difference between the two averages is most likely due to sample-specific parameters such as different drip rates or degrees of cave ventilation (Fairchild et al., 2006; Frisia et al., 2011). At about 890 ± 20 CE an abrupt increase in $\delta^{13}C$ begins. Over the next 100 years $\delta^{13}C$ increases by ~8‰ in both stalagmites (Fig. 5). For example, based on the age model of AB2 $\delta^{13}C$ values are still below −7‰ at 885 CE and rise to 0.62 at 1020 CE. The increase is slightly more rapid in AB3, with $\delta^{13}C$ values of −8.69 at 892 CE rising to +0.4 at 992 CE. After about 900 CE the $\delta^{13}C$ values continue to increase more slowly, with peak values of greater than 4‰ in both samples around 1800–2000 CE. A brief return to slightly negative values is seen around 1700 CE. The reproducibility of the shape, magnitude and timing of the $\delta^{13}C$ records in the two samples is a strong indication that the positive shift is driven by a regional change in the $\delta^{13}C$ values of dissolved inorganic carbon in the soil waters and not by sample-specific effects.

The oxygen isotope values of both samples vary mainly between −4 and −7‰ VPDB with values for AB2 enriched by 0.3–0.5 per mil compared to AB3. The 11-point running averages (approximately century scale) display similar trends in both samples (Fig. 5). From 500 to 900 CE, both oxygen isotope time series show a decrease in average values of about 1.5‰. After 900 CE average values increase by about 0.5‰ and remain relatively constant until about 1700 CE, then steadily increase by about 2‰ over the next 300 years. The carbon and oxygen isotope time series show no correlative shifts in isotopic values.

5. Discussion

The carbon isotope ratios of speleothem calcite reflect a mixture of three carbon sources: plant root-respired CO_2 in the soil zone, atmospheric CO_2, and dissolution of the host carbonate bedrock (McDermott, 2004). The carbon isotopic ratios of the latter two sources vary little, with CO_2 of preindustrial atmosphere having a $\delta^{13}C$ value of −6.5‰ (Leuenberger et al., 1992) and Eocene marine limestones such as that which hosts Anjohibe cave generally ranging from +1 to +2‰ (Shackleton, 1987). The $\delta^{13}C$ value of plant respired CO_2 varies primarily as a function of the photosynthetic pathway used by the plants. In landscapes dominated by plants photosynthesizing via the Calvin cycle (C_3 plants) – the great majority of temperate plants including trees and shrubs – plant-respired CO_2 averages approximately −26‰ VPDB (Farquhar et al., 1989). Plant root respiration also acidifies the soil water, which then equilibrates with the host bedrock and partially exchanges with the atmosphere. In such settings, typical $\delta^{13}C$ values for total dissolved inorganic carbon (DIC) in the groundwater and for speleothems growing beneath such landscapes lie between −8 and −12‰ VPDB (Fairchild et al., 2006; McDermott, 2004). In regions dominated by plants using the Hatch-Slack photosynthetic pathway (C_4 plants such as most dry region grasses), plant respired CO_2 averages about −14‰ VPDB (Farquhar et al., 1989). In these landscapes groundwater DIC and speleothem $\delta^{13}C$ values are enriched by 8–10‰ (Fairchild et al., 2006; McDermott, 2004) compared to regions overlain by C_3 plants. For our samples, the $\delta^{13}C$ values prior to 890 CE are typical for speleothems deposited in caves that are overlain by C_3-dominated ecosystems. Our data do not rule out the presence of C_4 grasses, but grasses likely made up less than 25% of the flora. Indeed, grass pollen are present in low percentages in lacustrine sediments in several areas of Madagascar well prior to 900 CE (Burney, 1987; Gasse and Van Campo, 1998).

We interpret the 8–10‰ enrichment in the carbon isotope values that occurs from 890 to 990 CE to be the result of a rapid, nearly complete transformation of the ecosystem in the surrounding region from one primarily composed of C_3 vegetation to one dominated by C_4 grasses with very little remnant C_3 vegetation. The $\delta^{13}C$ values of our samples after 990 CE are among the most enriched reported from speleothems. In particular, the $\delta^{13}C$ values of the past two centuries are enriched beyond what is to be expected from even complete C_4 ecosystems. We are not sure of the origin of such enriched values, but one possibility is that gradual drying of the region, as evidenced by a trend of increasing speleothem $\delta^{18}O$ over the past ~200 years, led to a gradual reduction in drip rate. A decreased drip rate would allow more extensive degassing of isotopically depleted CO_2 leading to more enriched speleothem $\delta^{13}C$ values. In any case, the C_4-dominated ecosystem has remained constant over the past ~950 years and comprises the modern landscape. Supporting evidence for our interpretation comes from carbon isotopic analyses of vertebrate bone collagen from fossils in Anjohibe Cave. Extinct taxa that lived in this region before 500 CE have average collagen $\delta^{13}C$ values of −23‰,

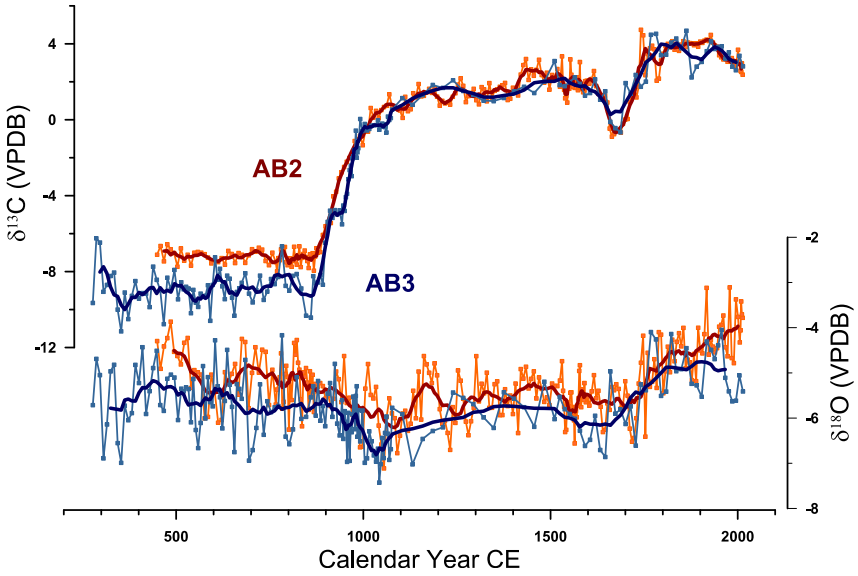

Fig. 5. Stable isotope time series. Time series of oxygen and carbon stable isotope ratios for stalagmites AB2 (orange) and AB3 (blue) from Anjohibe Cave, Madagascar. The age scale is in calendar years in the Common Era (CE).

indicating a C_3 plant diet, while more recently introduced taxa (rats and shrews) have $\delta^{13}C$ values of −15‰ and higher, indicating an almost exclusively C_4 diet (Crowley and Samonds, 2013).

Together with environmental indicators from lakes in the region, our results further suggest that the landscape transformation was the result of the expansion of the use of fire as a means of increasing the new growth of grass as forage for cattle. Sediments from lakes across Madagascar, including Kavitaha, Tritrivakely, Mitsinjo and Amparihibe, show marked increases in charcoal and Gramineae pollen percentages sometime between 700 and 1100 CE (Burney, 1987; Burney et al., 2004; Gasse and Van Campo, 1998; Matsumoto and Burney, 1994). These studies indicate important links between landscape burning and grassland expansion, but they do not provide precise estimates of the timing and rate of landscape change, nor have their proxy data allowed quantitative estimates of the increase in grass abundance. Our results place tight constraints on the timing of these changes, indicate that they occurred over a short time interval between 890 and 990 CE, and demonstrate that a complete floral succession from a dominantly forested landscape to the present palm savannah grassland took place in northwestern Madagascar at that time.

Burney et al. (2003) note increases in *Sporormiella*, a fungus found on the dung of large herbivores, in Lakes Kavitaha and Amparihibe at approximately the same time as the increase in charcoal and grass pollen abundance. We posit that the introduction of *Bos indicus* during the middle to late first millennium (Allibert et al., 1989; Beaugard, 2011; Burney et al., 2003; Fuller and Boivin, 2009) resulted in a shift in human economy from dominant foraging (with its greater dependence on bushmeat hunting and wild plant collecting) to a dedicated agro-pastoralist subsistence strategy, as seen at early large settlement sites such as Irodo (Dewar and Wright, 1993) and Mahilaka (Radimilahy, 1998). The changes in land use led to major habitat modification including major loss or fragmentation of existing forest. Our results suggest that C_3 dominated forest remained widespread prior to 900 CE, but was rapidly reduced in extent thereafter. The loss of forest habitat could only have increased the environmental pressure on remaining endemic species that rely on relatively connected forest cover for survival.

Prior assessments of the paleohabitat in the region of Anjohibe have been based on limited data. Burney et al. (1997) suggested that palm savannah might have existed in the region over the past 40,000 years. This assessment, however, derives from only six analyses of pollen contained in speleothems from Anjohibe, of which two were undated, three were deemed securely dated, and one (the most recent) less securely dated at under four thousand years old (Burney et al., 1997). All six samples contain endemic palm and grasses, both of which still occur in the region, together with other trees and shrubs, though in low quantities (Burney et al., 1997). We can infer with confidence, however, that other trees and shrubs were well represented in the area before the megafauna disappeared because of the nature of the vertebrate subfossil assemblage in the cave, which included *Prolemur simus*, *Palaeopropithecus kelyus*, and *Babakotia radofilai* (Godfrey et al., 1999) with known arboreal locomotor habits and food preferences (Jungers et al., 2002).

Although humans are generally thought to be the primary cause of the loss of Madagascar's endemic species recent studies of the decline of forest cover have suggested that climate change may have also played an important role. In particular, periods of drought may have been the primary or at least complementary cause of the forest loss, grassland expansion and megafauna disappearance across Madagascar (Virah-Sawmy et al., 2010). The oxygen isotope results from our work provide important data that can address this question. Oxygen isotope ratios of speleothem calcite are primarily controlled by two factors: cave temperature through the temperature dependence of the fractionation between water and calcium carbonate minerals, and the isotopic composition of rainfall (Lachniet, 2009). Tropical temperature variability in the study region over the past 2000 years was likely on the order of one degree C (Weldeab et al., 2014), which would result in 0.25‰ variation in speleothem $\delta^{18}O$. Thus, the primary driver of changes in speleothem oxygen isotope variability in our samples is the isotopic composition of precipitation.

In tropical regions dominated by summer convective rainfall, interannual changes in $\delta^{18}O$ of rainfall and of speleothem calcite are inversely correlated with regional precipitation (Bony et al., 2008; Rozanski et al., 1993). Our oxygen isotope time series, while

displaying up to 2 per mille variability on decadal and centennial timescales, shows no monotonic trend over the past 1500 years. Importantly, the $\delta^{18}O$ values of our samples do not increase at the time of the very large shift in $\delta^{13}C$ and, therefore, do not indicate a climatic shift to drier conditions at the time of the inferred ecosystem shift. If anything, the decreasing trend in $\delta^{18}O$ suggests a trend of increasing rainfall before and continuing briefly after the observed large carbon isotope shift. We thank the Department of Paleontology and Biological Anthropology at the University of Antananarivo, Madagascar, for its help in facilitating this research.

6. Conclusions

Stable isotopic time series from two well-dated speleothems from Anjohibe Cave in northwestern Madagascar provide insights into the paleoecology and paleoclimate of the region over the past 1800 years. From 300 CE to 890 CE the vegetation of the region was dominated by plants using the C_3 photosynthetic pathway, and is interpreted to have been an open forest landscape with a minor component of C_4 grasses. Beginning at 890 CE and over the course of the next 100 years the region changed to one heavily dominated by C_4 grasses, similar to the modern landscape.

Rather than climate, our results suggest that human activity, specifically expanded use of fire to produce fodder for cattle, resulted in rapid loss of forest habitat. These changes very likely increased environmental pressures on Madagascar's megafauna and accelerated their disappearance.

Acknowledgements

This research was partially supported by funding from the University of Massachusetts Natural History Collections (LRG). DM acknowledges support from NSF award EAR-1439559 and the MIT Ferry Fund. We greatly appreciate the support and cooperation of the Madagascar Ministry of Art and Culture, Ministry of Mines and Petroleum and Ministry of Higher Education and Scientific Research in sample collection.

References

Allibert, C., Argant, A., Argant, J., 1989. Le site archéologique de Dembeni (Mayotte), Archipel des Comores. Etudes Océan Indien 11, 61–172.

Beaugard, P., 2011. The first migrants to Madagascar and their introduction of plants: linguistic and ethnological evidence. Azania Archaeol. Res. Afr. 46, 169–189.

Besairie, H., Collignon, M., 1972. Géologie de Madagascar, 1. Les terrains sedimentaires. Ann. Géologiques Madag 35, 1–463.

Bond, W.J., Silander Jr., J.A., Ranaivonasy, J., Ratsirarson, J., 2008. The antiquity of Madagascar's grasslands and the rise of C_4 grassy biomes. J. Biogeogr. 35, 1743–1758. http://dx.doi.org/10.1111/j.1365-2699.2008.01923.x.

Bony, S., Risi, C., Vimeux, F., 2008. Influence of convective processes on the isotopic composition ($\delta^{18}O$ and δD) of precipitation and water vapor in the tropics: 1. Radiative-convective equilibrium and Tropical Ocean–Global Atmosphere–Coupled Ocean-Atmosphere Response Experiment (TOGA-COARE) simulations. J. Geophys. Res. Atmos. 113, D19305. http://dx.doi.org/10.1029/2008JD009942.

Burney, D.A., 1987. Late Holocene vegetational change in central Madagascar. Quat. Res. 28, 130–143. http://dx.doi.org/10.1016/0033-5894(87)90038-X.

Burney, D.A., Burney, L.P., Godfrey, L.R., Jungers, W.L., Goodman, S.M., Wright, H.T., Jull, A.J.T., 2004. A chronology for late prehistoric Madagascar. J. Hum. Evol. 47, 25–63. http://dx.doi.org/10.1016/j.jhevol.2004.05.005.

Burney, D.A., Robinson, G.S., Burney, L.P., 2003. Sporomiella and the Late Holocene extinctions in Madagascar. Proc. Natl. Acad. Sci. 100, 10800–10805. http://dx.doi.org/10.1073/pnas.1534700100.

Burney, D., James, H., Grady, F., Rafamantanantsoa, J.-G., Ramilisonina, Wright, H., Cowart, J., 1997. Environmental change, extinction and human activity: evidence from caves in NW Madagascar. J. Biogeogr. 24, 755–767. http://dx.doi.org/10.1046/j.1365-2699.1997.00146.x.

Cheng, H., Adkins, J., Edwards, R.L., Boyle, E.A., 2000. U-Th dating of deep-sea corals. Geochim. Cosmochim. Acta 64, 2401–2416. http://dx.doi.org/10.1016/S0016-7037(99)00422-6.

Cheng, H., Lawrence Edwards, R., Shen, C.-C., Polyak, V.J., Asmerom, Y., Woodhead, J., Hellstrom, J., Wang, Y., Kong, X., Spötl, C., Wang, X., Calvin Alexander Jr., E., 2013. Improvements in ^{230}Th dating, ^{230}Th and ^{234}U half-life values, and U–Th isotopic measurements by multi-collector inductively coupled plasma mass spectrometry. Earth Planet. Sci. Lett. 371–372, 82–91. http://dx.doi.org/10.1016/j.epsl.2013.04.006.

Crowley, B.E., 2010. A refined chronology of prehistoric Madagascar and the demise of the megafauna. Quat. Sci. Rev., Special Theme Case Stud. Neodymium Isotopes Paleoceanogr. 29, 2591–2603. http://dx.doi.org/10.1016/j.quascirev.2010.06.030.

Crowley, B.E., Samonds, K.E., 2013. Stable carbon isotope values confirm a recent increase in grasslands in northwestern Madagascar. Holocene 23, 1066–1073. http://dx.doi.org/10.1177/0959683613484675.

Dewar, R.E., Wright, H.T., 1993. The culture history of Madagascar. J. World Prehistory 7, 417–466. http://dx.doi.org/10.1007/BF00997802.

Fairchild, I., Smith, C., Baker, A., Fuller, L., Spotl, C., Mattey, D., McDermott, F., EIMP, 2006. Modification and preservation of environmental signals in speleothems. Earth Sci. Rev. 75, 105–153. http://dx.doi.org/10.1016/j.earscirev.2005.08.003.

Farquhar, G.D., Ehleringer, J.R., Hubick, K.T., 1989. Carbon isotope discrimination and photosynthesis. Annu. Rev. Plant Physiol. Plant Mol. Biol. 40, 503–537. http://dx.doi.org/10.1146/annurev.pp.40.060189.002443.

Frisia, S., Fairchild, I.J., Fohlmeister, J., Miorandi, R., Spötl, C., Borsato, A., 2011. Carbon mass-balance modelling and carbon isotope exchange processes in dynamic caves. Geochim. Cosmochim. Acta 75, 380–400. http://dx.doi.org/10.1016/j.gca.2010.10.021.

Fuller, D.Q., Boivin, N., 2009. Crops, cattle and commensals across the Indian Ocean. Etudes Océan Indien 43–43, 13–46.

Gade, D.W., 1996. Deforestation and its effects in highland Madagascar. Mt. Res. Dev. 16, 101–116. http://dx.doi.org/10.2307/3674005.

Gasse, F., Van Campo, E., 1998. A 40,000-yr pollen and diatom record from Lake Tritrivakely, Madagascar, in the Southern Tropics. Quat. Res. 49, 299–311. http://dx.doi.org/10.1006/qres.1998.1967.

Godfrey, L.R., Jungers, W.L., Simons, E.L., Chatrath, P.S., Rakotosamimanana, B., 1999. Past and present distributions of lemurs in Madagascar. In: Rakotosamimanana, B., Rasamimanana, H., Ganzhorn, J.U., Goodman, S.M. (Eds.), New Directions in Lemur Studies. Kluwer, New York, pp. 19–53.

Humbert, H., 1927. Destruction d'une flore insulaire par les feux: principaux aspects de la végétation à Madagascar. Mém. L'Académie Malgache 5, 1–80.

Jaffey, A.H., Flynn, K.F., Glendenin, L.E., Bentley, W.C., Essling, A.M., 1971. Precision measurement of half-lives and specific activities of ^{235}U and ^{238}U. Phys. Rev. C 4, 1889–1906. http://dx.doi.org/10.1103/PhysRevC.4.1889.

Jarosz, L., 1993. Defining and explaining tropical deforestation: shifting cultivation and population growth in Colonial Madagascar (1896-1940). Econ. Geogr. 69, 366–379. http://dx.doi.org/10.2307/143595.

Jungers, W.L., Godfrey, L.R., Simons, E.L., Wunderlich, R.E., Richmond, B.G., Chatrath, P.S., 2002. Ecomorphology and behavior of giant extinct lemurs from Madagascar. In: Plavcan, J.M., Kay, R.F., Jungers, W.L., van Schaik, C.P. (Eds.), Reconstructing Behavior in the Primate Fossil Record. Kluwer, pp. 371–411.

Klein, J., 2002. Deforestation in the Madagascar highlands – established 'truth' and scientific uncertainty. GeoJournal 56, 191–199. http://dx.doi.org/10.1023/A:1025187422687.

Kull, C.A., 2000. Deforestation, erosion, and fire: degradation myths in the environmental history of Madagascar. Environ. Hist. 6, 423–450. http://dx.doi.org/10.3197/096734000129342361.

Lachniet, M.S., 2009. Climatic and environmental controls on speleothem oxygen-isotope values. Quat. Sci. Rev. 28, 412–432.

Leuenberger, M., Siegenthaler, U., Langway, C., 1992. Carbon isotope composition of atmospheric CO_2 during the last ice age from an Antarctic ice core. Nature 357, 488–490. http://dx.doi.org/10.1038/357488a0.

Ludwig, K.R., 1993. UISO; a Program for Calculation of ^{230}Th-^{234}U-^{238}U Isochron Ages (USGS Numbered Series No. 93–531). Open-File Report. U.S. Geological Survey.

Matsumoto, J., Burney, D.A., 1994. Late Holocene environments at Lake Mitsinjo, northwestern Madagascar. Holocene 4, 16–24. http://dx.doi.org/10.1177/095968369400400103.

Mayaux, P., Gond, V., Bartholomé, E., 2000. A near real-time forest cover map of Madagascar derived from spot vegetation data. Int. J. Remote Sens. 21, 3139–3144.

McConnell, W.J., Kull, C.A., 2014. Deforestation in Madagascar: debates over the island's forest cover and challenges of measuring forest change. In: Conservation and Environmental Management in Madagascar. Routledge, London, pp. 67–104.

McDermott, F., 2004. Palaeo-climate reconstruction from stable isotope variations in speleothems: a review. Quat. Sci. Rev. 23, 901–918.

McGee, D., Quade, J., Edwards, R.L., Broecker, W.S., Cheng, H., Reiners, P.W., Evenson, N., 2012. Lacustrine cave carbonates: novel archives of paleohydrologic change in the Bonneville Basin (Utah, USA). Earth Planet. Sci. Lett. 351–352, 182–194. http://dx.doi.org/10.1016/j.epsl.2012.07.019.

Perrier de la Bâthie, H., 1921. La végétation malgache. Ann. Mus. Colon. Marseille 9, 1–266.

Quéméré, E., Amelot, X., Pierson, J., Crouau-Roy, B., Chikhi, L., 2012. Genetic data suggest a natural prehuman origin of open habitats in northern Madagascar and question the deforestation narrative in this region. Proc. Natl. Acad. Sci. 109, 13028–13033. http://dx.doi.org/10.1073/pnas.1200153109.

Radimilahy, C., 1998. Mahilaka: an archaeological investigation of an early town in northwestern Madagascar. Uppsala. In: Studies in African Archaeology, 15,

p. 293, 165 figs., 38 plates. ISSN 0284-5040, ISBN 91-506-1313-8.
Rozanski, K., Araguás-Araguás, L., Gonfiantini, R., 1993. Isotopic patterns in modern global precipitation. In: Climate Change in Continental Isotopic Records. American Geophysical Union.
Shackleton, N.J., 1987. The carbon isotope record of the Cenozoic: history of organic carbon burial and of oxygen in the ocean and atmosphere. Geol. Soc. Lond. Spec. Publ. 26, 423–434. http://dx.doi.org/10.1144/GSL.SP.1987.026.01.27.
Virah-Sawmy, M., Willis, K.J., Gillson, L., 2010. Evidence for drought and forest declines during the recent megafaunal extinctions in Madagascar. J. Biogeogr. 37, 506–519. http://dx.doi.org/10.1111/j.1365-2699.2009.02203.x.
Weldeab, S., Lea, D.W., Oberhänsli, H., Schneider, R.R., 2014. Links between south-western tropical Indian Ocean SST and precipitation over southeastern Africa over the last 17 kyr. Palaeogeogr. Palaeoclimatol. Palaeoecol. 410, 200–212. http://dx.doi.org/10.1016/j.palaeo.2014.06.001.